

Original Research

A Predictive Model Based on the FBXO Family Reveals the Significance of Cyclin F in Hepatocellular Carcinoma

Dute $Gao^{1,2,3}$, Suxin $Li^{1,2,3}$, Huahu $Guo^{1,2,3}$, Xianfu $Liu^{1,2,3}$, Zhaochen $Liu^{1,2,3}$, Luhao $Li^{1,2,3}$, Liang $Bao^{1,2,3}$, Xiaowei $Dang^{1,2,3,*}$

Academic Editor: Amancio Carnero Moya

Submitted: 15 December 2023 Revised: 15 March 2024 Accepted: 28 March 2024 Published: 24 May 2024

Abstract

Objective: The F-box protein (FBXO) family plays a key role in the malignant progression of tumors. However, the biological functions and clinical value of the FBXO family in liver cancer remain unclear. Our study comprehensively assessed the clinical value of the FBXO family in hepatocellular carcinoma (HCC) and constructed a novel signature based on the FBXO family to predict prognosis and guide precision immunotherapy. **Methods**: The Cancer Genome Atlas (TCGA) and International Cancer Genome Consortium (ICGC) databases were utilized to investigate the expression characteristics and prognostic value of the FBXO family in HCC. A predictive model based on the FBXO family using TCGA database; and its predictive ability was validated using the ICGC database. Further analyses revealed that this predictive model can independently predict the overall survival (OS) rate of patients with HCC. We further analyzed the association of this predictive model with signaling pathways, clinical pathological features, somatic mutations, and immune therapy responses. Finally, we validated the biological functions of cyclin F (*CCNF*) through *in vitro* experiments. **Results**: A predictive model involving three genes (*CCNF*, *FBXO43*, and *FBXO45*) was constructed, effectively identifying high and low-risk patients with differences in OS, clinicopathological characteristics, somatic mutations, and immune cell infiltration status. Additionally, knock-down of *CCNF* in HCC cell lines reduced cell proliferation *in vitro*, suggesting that *CCNF* may be a potential therapeutic target for HCC. **Conclusions**: The predictive model based on the FBXO family can effectively predict OS and the immune therapy response in HCC. Additionally, *CCNF* is a potential therapeutic target for HCC.

Keywords: FBXO family; hepatocellular carcinoma; prognostic value; immunotherapy response; cyclin F

1. Introduction

According to the 2020 cancer statistics from the World Organization for Research on Cancer, hepatocellular carcinoma (HCC) is the fifth most common cancer globally and the second leading cause of cancer-related deaths in males [1]. For early-stage HCC patients, surgical resection remains the primary treatment choice; however, more than 70% of patients experience recurrence after surgical treatment [2]. Early-stage HCC typically presents without noticeable symptoms, contributing to its covert onset. Consequently, most HCC patients present with symptoms at an advanced stage of disease, rendering them unsuitable for surgical treatment [3,4]. Despite substantial efforts over the past few decades to improve the screening, diagnosis, and treatment of HCC, only 9% of HCC patients survive for more than 5 years [5]. Immune checkpoint inhibitors have emerged as a novel therapeutic approach for liver cancer and have shown some effectiveness in the clinical treatment of liver cancer patients; however, this treatment method has proven beneficial for only a minority of patients in clinical

practice [6]. Therefore, it is essential to identify precise diagnostic and prognostic biomarkers for HCC.

The ubiquitin proteasome system is a highly selective proteolytic system that controls the protein degradation process and plays an important role in cancer development [7]. F-box (FBXO) proteins are the core component of the S phase kinase-associated protein 1-cullin 1-FBXO E3 ubiquitin ligase family [8]. The FBXO family, which regulates numerous cellular biological processes and signaling pathways linked to malignancies, holds great significance [9]. For example, FBXO1 is involved in DNA repair and genome stability [10]. FBXO5 stabilizes substrates to regulate the cell cycle [11]. FBXO28 may exert tumor-promoting effects on breast cancer via the ubiquitination of Myc143, inducing transcription. Nevertheless, the value and biological function of the FBXO family in HCC remain unclear and require further elucidation.

Within the FBXO family, FBXO1, FBXO18, FBXO23, and FBXO29 are also known as cyclin F (CCNF), F-box DNA helicase 1, Tetraspanin-17 and

¹Department of Hepatopancreatobiliary Surgery, The First Affiliated Hospital of Zhengzhou University, 450000 Zhengzhou, Henan, China

²Key Laboratory of Precision Diagnosis and Treatment in General Surgical (Hepatobiliary and Pancreatic) Diseases of Health Commission of Henan Province, 450000 Zhengzhou, Henan, China

³Henan Province Engineering Research Center of Minimally Invasive Diagnosis and Treatment of Hepatobiliary and Pancreatic Diseases, 450000 Zhengzhou, Henan, China

^{*}Correspondence: dangxw1001@zzu.edu.cn (Xiaowei Dang)

F-box/WD repeat-containing protein 8, respectively. In this study, we established a predictive model based on the FBXO family through comprehensive bioinformatics analysis, and its accuracy and reliability were internally and externally validated. Additionally, we evaluated the diagnostic and prognostic value of this model. Finally, we validated the biological functions of *CCNF*. Our results indicate that the predictive model based on the FBXO family is instrumental in improving personalized prognosis prediction and precise immunotherapy. Furthermore, cyclin F was identified as a potential therapeutic target for HCC.

2. Materials and Methods

2.1 Data Collection and HCC Sample Acquisition

High-throughput transcriptome sequencing mRNA expression matrix and corresponding clinicopathological information of HCC patients were obtained from International Cancer Genome Consortium (ICGC) (https://dcc.ic gc.org/) website and The Cancer Genome Atlas (TCGA) (https://portal.gdc.cancer.gov/) [12]. For TCGA dataset, 371 HCC patients were utilized as the training cohort. The validation cohort, consisting of 231 Japanese patients with HCC, was derived from the ICGC dataset. eight fresh HCC tissues were collected from the First Affiliated Hospital of Zhengzhou University for analysis. All patients with HCC included in this study were initially diagnosed with HCC for the first time and did not receive any treatment before surgery. They were all pathologically diagnosed with HCC, provided written informed consent, allowing us to obtain clinical samples. This study obtained approval from the Ethics Committee of the First Affiliated Hospital of Zhengzhou University. All samples were stored in a low-temperature freezer at -80 °C.

2.2 Analysis of FBXO Family Expression Data

We analyzed the gene expression matrix of the FBXO family in 371 HCC tumor samples and their corresponding liver tissues using the Gene Expression Profiling Interactive Analysis (GEPIA) database [13]. The "maftools" software was employed to assess and present the mutation data of different groups, with each gene mutation depicted using waterfall charts. To evaluate immune cell enrichment scores, the single-sample gene set enrichment analysis (ssGSEA) approach was employed, facilitated by the "Gene Set Variation Analysis" R package (v1.40.1). Spearman's analysis was utilized to assess the relationship between the model and immunological infiltration, and the findings were visualized using lollipop charts. A comparison was made between the model and immunological checkpoint data. Tumor Immune Dysfunction and Exclusion (TIDE) analysis is used to predict the efficacy of immunotherapy in HCC patients [14].

2.3 Functional Analysis

We utilized the "clusterProfiler" R package (v4.2.2) to conduct GSEA with the aim of identifying potential biological roles and signaling pathways among different subgroups. Pathways with p value < 0.05 were considered significantly enriched.

2.4 Development and Validation of the FBXO Prognostic Model

The "DESeq2" R program was utilized initially to analyze the mRNA expression matrix from TCGA dataset. If the genes met the following criteria, they were considered differentially expressed genes (DEGs): |fold change| >1.5 and adjusted p < 0.05. Univariate Cox regression analysis was employed to identify the predictive genes. A risk score based on the FBXO family was evaluated based on the expression levels of overall survival (OS)-related FBXO genes, which were included in the multiple regression model. The regression coefficient (β) was used to quantify the impact of these genes on the risk score (RS) = expression of $FBXO45 \times 0.2609 + \text{expression}$ of $FBXO43 \times 0.3369 + \text{expression}$ of $CCNF \times 0.3369$.

2.5 5-Ethynyl-2'-deoxyuridine (EdU) Cell Proliferation Assay

The EdU cell proliferation assay was conducted using an EdU assay kit (Abbkine, Wuhan, China) following the manufacturer's protocol. Cells were seeded in 96-well plates at a density of 3×10^3 cells per well. The next day, cells were treated with 10 μM EdU and incubated for 2 h. Subsequently, the cells were fixed, permeabilized, and incubated with 150 μL Click-iT reaction mixture for 30 min. Cell visualization was performed by fluorescence microscopy.

2.6 Colony Formation Assay and the Cell Counting Kit-8 Assay

The Cell Counting Kit-8 (CCK-8) assay, which measures cell proliferation, was performed using a CCK-8 kit (CK04; Dojindo Molecular Technologies, Inc., Rockville, MD, USA). For HCC cell culture, 3×10^3 cells per well were seeded in 96-well plates. Each well received 10 μ L CCK-8 solution and was incubated for 2 h, after which the absorbance was measured. Additionally, 1×10^3 HCC cells were seeded into 12- or 24-well plates. After 10 days of incubation, the media was removed and the cells were fixed in 4% paraformaldehyde (C8; Solarbio Life Science, Beijing, China) for 30 min, followed by staining with a 0.1% crystal violet solution.

2.7 Quantitative Real-Time PCR (qRT-PCR) and Western Blotting (WB)

Total RNA was extracted from HCC tissues (CW3166; CoWin Biosciences, Cambridge, MA, USA) following standard protocols [15]. Then the extracted total



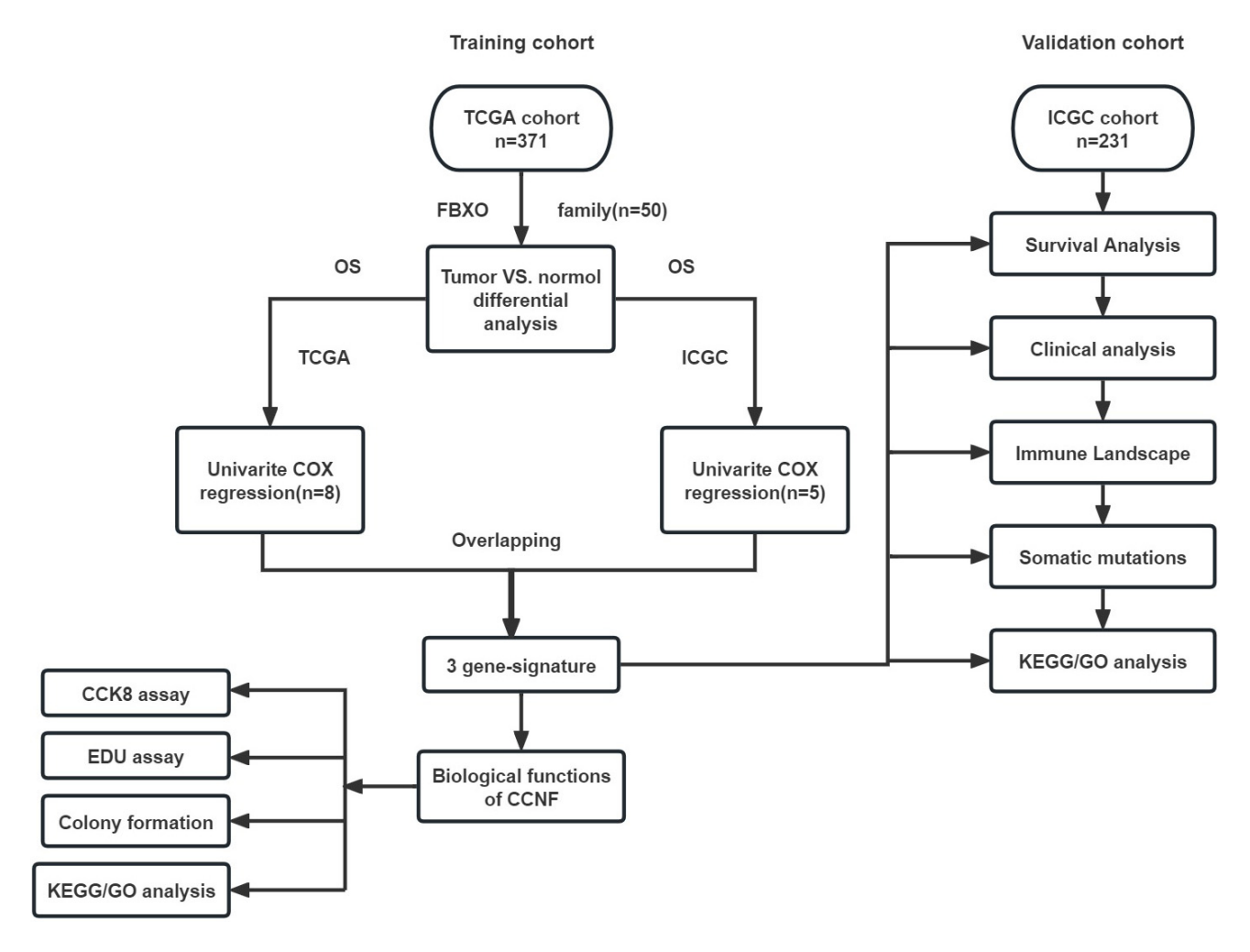


Fig. 1. Flowchart for this study. TCGA, The Cancer Genome Atlas; FBXO, F-box protein; OS, overall survival; ICGC, International Cancer Genome Consortium; COX, cox proportional hazards regression; CCK8, cell counting kit-8; EDU, 5-ethynyl-2'-deoxyuridine; KEGG, kyoto encyclopedia of genes and genomes; GO, gene ontology; CCNF, cyclin F.

mRNAs were reversely transcribed using HiScript III RT SuperMix (Vazyme, Nanjing, China). qRT-PCR was carried out on the QuantStudio3 Real-Time PCR System using the YBR qPCR Master Mix (Vazyme). GAPDH was employed for standard normalization. The primer sequences utilized for amplification are listed in **Supplementary Table 1**. Western Blotting was performed as previously described [16]. Primary antibodies against CCNF (864429) was acquired from Zenbio. Antibodies against GAPDH (60004-1-Ig) was obtained from Proteintech.

2.8 Cell Culture and Small Interfering RNA Transfection

Human HCC cell lines (HepG2, Huh7, MHCC-97H, SMMC-7721) were obtained from the Chinese Academy of Sciences (Shanghai, China) and cultured in Dulbecco's Modified Eagle Medium at 37 °C in a humid atmosphere of 95% air and 5% CO₂. All cell lines were validated by short tandem repeat (STR) profiling and tested negative for mycoplasma. Small interfering RNA (siRNA) target sequences for CCNF were as follows: si-CCNF, sense:

5'-TCAGGCCAGGAAGTCATGTTT-3'; negative control (NC), sense: 5'- UUCUCCGAACGUGUCACGUTT-3'. The efficiency of siRNA was evaluated by qPCR.

2.9 Statistical Analyses

Statistical analyses were performed using the R program (version 4.1.1, https://www.r-project.org). Group differences were evaluated using either analysis of variance or the Student's t-test. Cox proportional hazards regression analysis was employed to identify risk factors, and p < 0.05 was considered statistically significant.

3. Results

3.1 Construction of the FBXO Prognostic Model

We created a flowchart to outline the main approach of this study (Fig. 1). The study included a total of 50 FBXO family members, with 26 genes identified as DEGs between HCC and normal liver tissues (Fig. 2A). Subsequent univariate analysis identified eight prognosis-related genes in the TCGA database and five genes in the ICGC



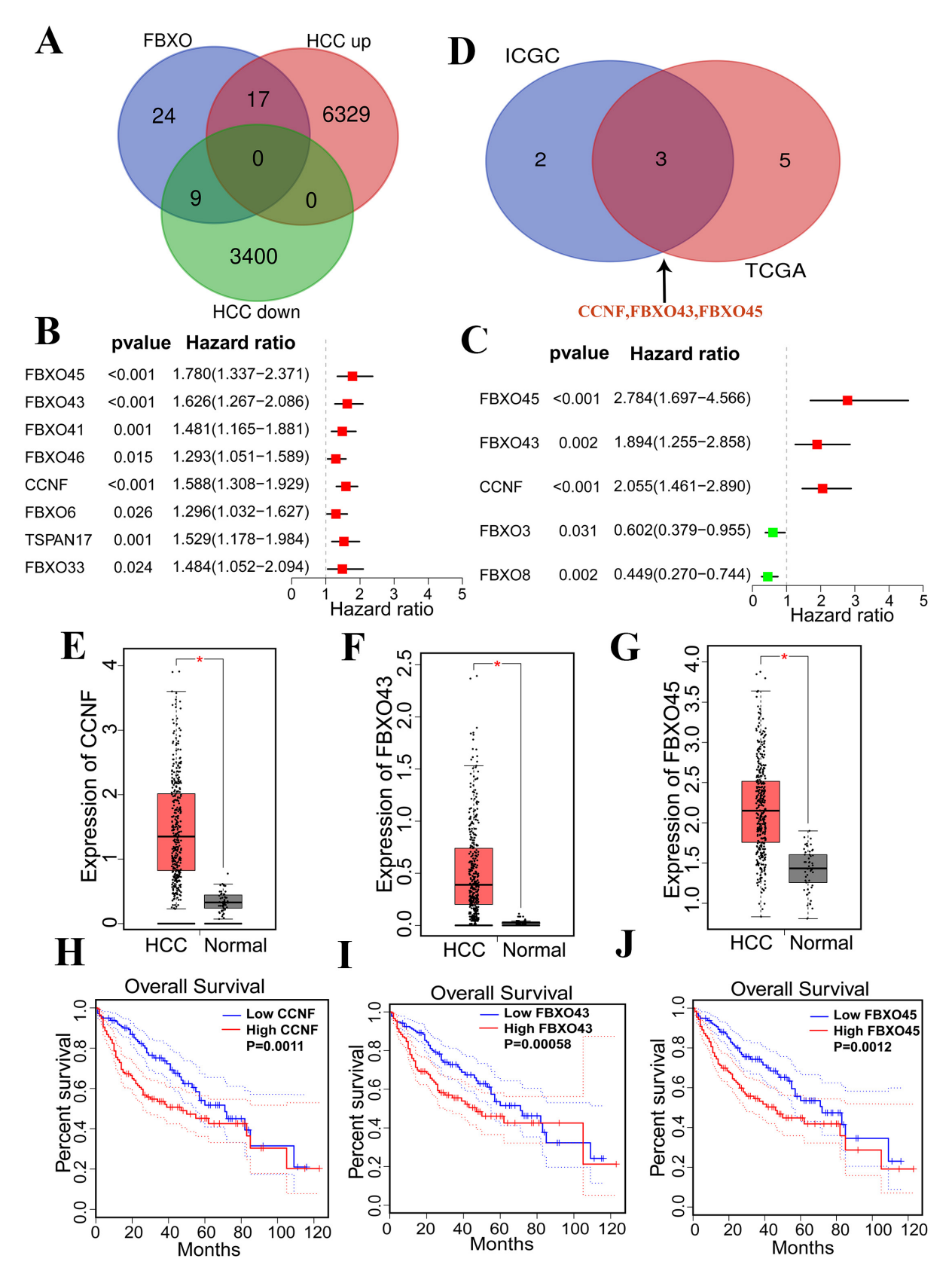


Fig. 2. Identification of key genes in the FBXO family. (A) A venn diagram showed that 26 abnormal expressed FBXO family in TCGA dataset. (B,C) Univariate Cox regression analysis of OS proved that several hub FBXO family were prognostic biomarkers in TCGA (B) and ICGC (C) datasets. (D) A Venn diagram reveals that CCNF, FBXO43, and FBXO45 are key prognostic genes. (E–G) FBXO43, CCNF, and FBXO45 are re highly expressed in HCC. (H–J) High expression of CCNF, FBXO43 or FBXO45 is associated with poor prognosis in HCC patients. HCC, hepatocellular carcinoma. *p < 0.05.

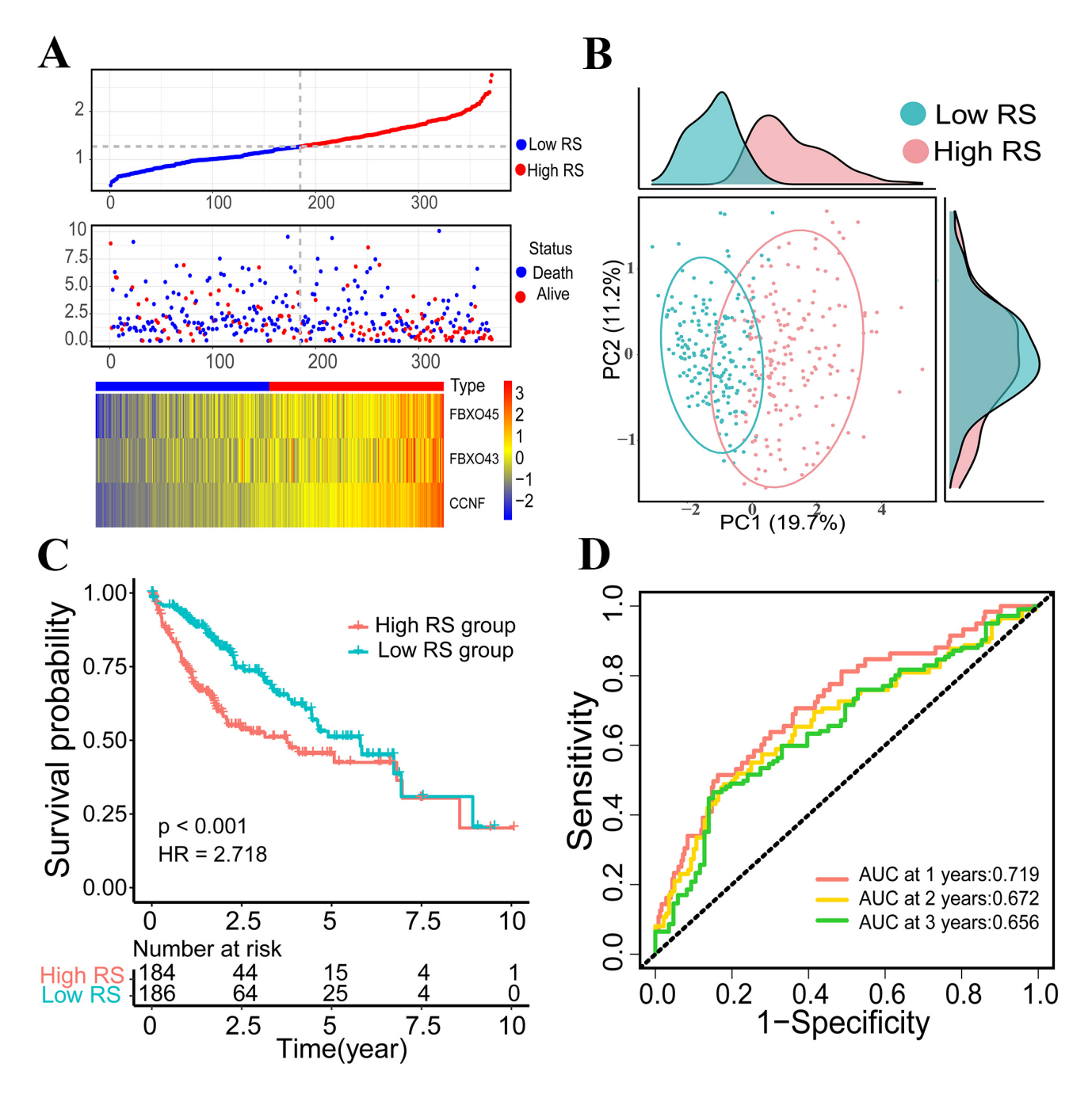


Fig. 3. Survival analysis of this model based on TCGA dataset. (A) Relationship between RS and survival status in HCC patients. (B) PCA plots of the high and low-RS groups. (C) Patients with high-RS had poor OS than low-RS group. (D) ROC curves of RS for predicting survival of patients with HCC. RS, risk score; PCA, Principal Component Analysis; ROC, Receiver Operating Characteristic.

database. Among them, *CCNF*, *FBXO43*, and *FBXO45* genes showed significant associations with the prognosis of HCC patients in both databases (TCGA database: *FBXO45*: $p = 7.988 \times 10^{-5}$, HR = 1.780 (1.336–2.371); *FBXO43*: $p = 1.360 \times 10^{-4}$, HR = 1.625 (1.266–2.086); *CCNF*: $p = 3.063 \times 10^{-6}$, HR = 1.588 (1.307–1.928); ICGC database: *FBXO45*: $p = 4.992 \times 10^{-5}$, HR = 2.784 (1.697–4.566); *FBXO43*: $p = 2.360 \times 10^{-3}$, HR = 1.893 (1.254–2.857); *CCNF*: $p = 3.458 \times 10^{-5}$, HR = 2.055 (1.461–2.890); Fig. 2B–D). We further conducted visual analysis

of the abnormal expression and prognostic correlation of the *FBXO43*, *FBXO45*, and *CCNF* using the online tools GEPIA in HCC (Fig. 2E–J). Due to the independent correlation of *CCNF*, *FBXO45*, and *FBXO43* expression with OS in both databases, we selected *CCNF*, *FBXO45*, and *FBXO43* to construct a predictive model. The risk score (RS) was calculated for each HCC patient based on the formula mentioned above. Using the median RS as the threshold, TCGA cohort was stratified into the high RS group consisting of 185 patients and the low RS group comprising



186 patients (Fig. 3A). As shown in Fig. 3C, HCC patients in the high RS group had shorter OS than those in the low RS group (log-rank test, p < 0.001, HR = 2.718 (1.809–4.085)). Higher risk scores were correlated with shorter survival time (Fig. 3A). The area under the curve (AUC) values for 1-, 2-, and 3-year OS were 0.719, 0.672, and 0.656, respectively (Fig. 3D). Principal component analysis (PCA) demonstrated a clear separation of patients into two subgroups (Fig. 3B).

3.2 Prognostic Model Validation in the ICGC Dataset

To further validate the accuracy of the predictive model, the ICGC cohort was included for model validation. (Fig. 4A). Consistent with the results of TCGA database, patients in the high RS group exhibited poorer OS (logrank test, p < 0.001, HR = 4.962 (2.444–10.074)) (Fig. 4C). The AUC values for 1-, 2-, and 3-year OS of RS in the ICGC database were 0.744, 0.704, and 0.725, respectively (Fig. 4D). These results demonstrate the reliability of the RS in predicting the OS of HCC patients. Additionally, PCA revealed distinct patient clustering in the two subgroups (Fig. 4B).

3.3 Correlations between the RS and Clinical Characteristics

We analyzed the relationship between RS and clinicopathological parameters. As shown in Table 1, highrisk patients exhibited significantly advanced tumor-nodemetastasis (TNM) staging (p=0.016), poorer histological differentiation (p<0.001), older age (p=0.013), and higher alpha-fetoprotein (AFP) levels (p=0.001). These findings suggest a tendency for high-risk patients to have unfavorable clinical characteristics.

We further conducted univariate analysis in TCGA cohort, including RS, age, sex, gender, TNM staging, tumor status, AFP, and vascular invasion. The results showed that TNM stage (HR = 2.449 (1.689–3.549), p < 0.05), tumor status (HR = 2.346 (1.610–3.419), p < 0.05), and RS (HR = 2.718 (1.809-4.085), p < 0.05) were associated with OS (Fig. 5A). Multivariate analysis further verified the independent correlation of RS with OS (HR = 2.327 (1.073-5.047), p = 0.033) (Fig. 5B). Univariate analysis in the ICGC database further revealed that TNM stage (HR = 2.492 (1.351-4.599), p < 0.001), RS (HR = 4.962 (2.444-1.599))10.074), p = 0.001), and sex (HR = 0.502 (0.268–0.940), p= 0.031) were closely associated with the OS of HCC patients (Fig. 5C). Multivariate analysis also indicated that RS (HR = 4.866 (2.365–10.011), p < 0.001) was an independent biomarker for HCC (Fig. 5D). Therefore, our research findings indicate that the model based on the FBXO family was independently correlated with the OS of HCC patients.

Table 1. Correlation between RS and clinicopathological characteristics of HCC patients*.

- Characteristics of ITCC patients :				
Characteristics	N	RSlow	RS^{high}	p value
Age (years)				0.013
< 60	169	73	96	
≥60	201	113	88	
NA	1			
Gender				< 0.001
Female	195	130	65	
Male	176	56	120	
Grade				< 0.001
I+II	232	141	91	
III+IV	134	42	92	
NA				
TNM stage				0.016
I+ II	257	138	119	
III+IV	90	35	55	
NA	13			
AFP				
< 60	213	128	85	< 0.001
≥60	65	15	50	
NA	93			

*Data from TCGA dataset. TNM, tumornodemetastasis.

3.4 Somatic Mutation Landscape in Different Subgroups Based on the RS

The "maftools" tool was used to study the differences in somatic mutation landscapes between the high RS and low RS groups. The somatic mutation landscape between subgroups is visually represented using waterfall plots (Fig. 6A,B). In the low RS group, the top six mutated genes were catenin beta 1 (CTNNB1), titin (TTN), albumin (ALB), mucin 16 (MUC16), tumor protein p53 (TP53), and piccolo presynaptic cytomatrix protein (PCLO), whereas in the high RS group, the top six mutated genes were *TP53*, *TTN*, *CTNNB1*, *MUC16*, low-density lipoprotein receptor-related protein 1B, and ryanodine receptor 2 (Fig. 6A,B). Additionally, when comparing gene alterations in the high RS and low RS groups, it was observed that the mutation frequency of *TP53* and retinoblastoma protein genes was higher in the high RS group (Fig. 6C).

3.5 RS Predicts the Immune Landscape and Immunotherapy Responses

We employed ssGSEA to calculate the enrichment scores for 24 immune cell types, estimating the relative abundance of cell infiltration in the HCC microenvironment (Fig. 7A). As shown in Fig. 7A and **Supplementary Table 2**, eosinophils (r = -0.419, $p = 1.93 \times 10^{-17}$), neutrophils (R = -0.254, $p = 2.59 \times 10^{-6}$), CD56 bright natural killer cells (R = -0.196, $p = 8.41 \times 10^{-5}$), type 1 helper T cells (R = -0.21, $p = 5.49 \times 10^{-5}$), effector memory CD8 T cells (R = -0.156, P = 0.006), mast cells (R = -0.11, P = 0.021), ac-



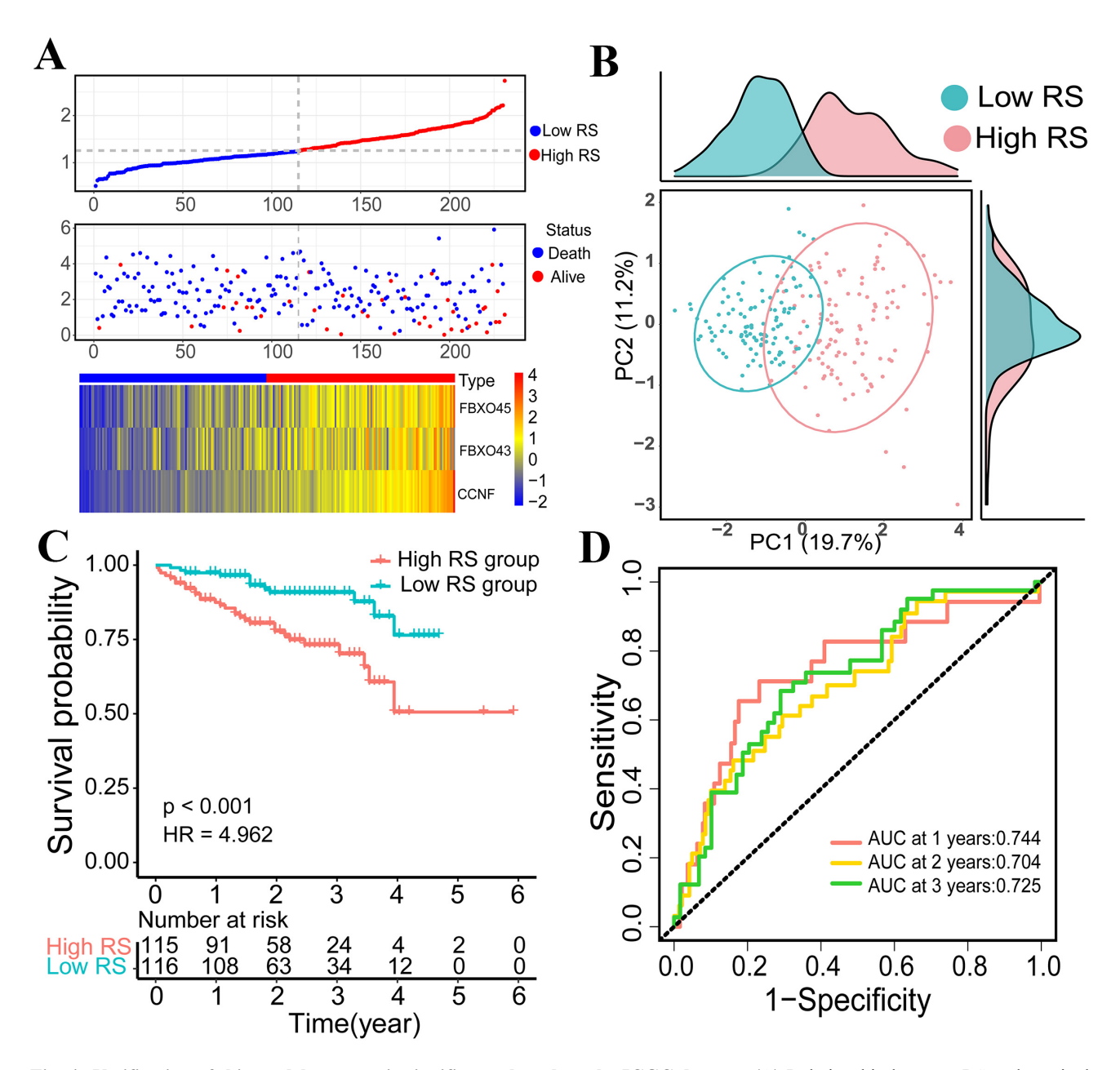


Fig. 4. Verification of this model prognostic significance based on the ICGC dataset. (A) Relationship between RS and survival status in HCC patients. (B) PCA plot of the high and low RS groups. (C) Survival analysis between high and low RS groups. (D) ROC curves of RS for predicting survival of patients with HCC.

tivated CD8 T cells (R = -0.150, p = 0.043), and CD56dim natural killer cells (R = -0.051, p = 0.043) were negatively correlated with RS. These findings suggest that high RS patients exhibit an immunosuppressive phenotype.

Fig. 7B shows that immune checkpoint molecules, including CD274, hepatitis A virus cellular receptor 2, lymphocyte activation gene 3, V-set immunoregulatory receptor, B- and T-lymphocyte attenuator, and T cell immunoreceptor with immunoglobulin and tyrosine-based inhibitory motif domain [17], were upregulated in the highrisk group. Furthermore, we conducted TIDE analysis and found that the high-risk group exhibited a significantly higher proportion of immunologically nonrespon-

sive individuals (64.9%), along with elevated TIDE ($p < 1.5 \times 10^{-13}$) and dysfunction scores ($p < 6.1 \times 10^{-11}$) (Fig. 7C,D). This suggests that the high-risk group might be more prone to immune escape and less responsive to immunotherapy.

3.6 Enriched Pathways and Functions between High- and Low- RS Groups

Supplementary Fig. 1B shows the 20 genes with the most significant differences between the high- and low-risk groups. To investigate the molecular mechanism of FBXO-mediated HCC development, we conducted Gene Ontology (GO) enrichment analysis and GSEA. GO analysis indi-



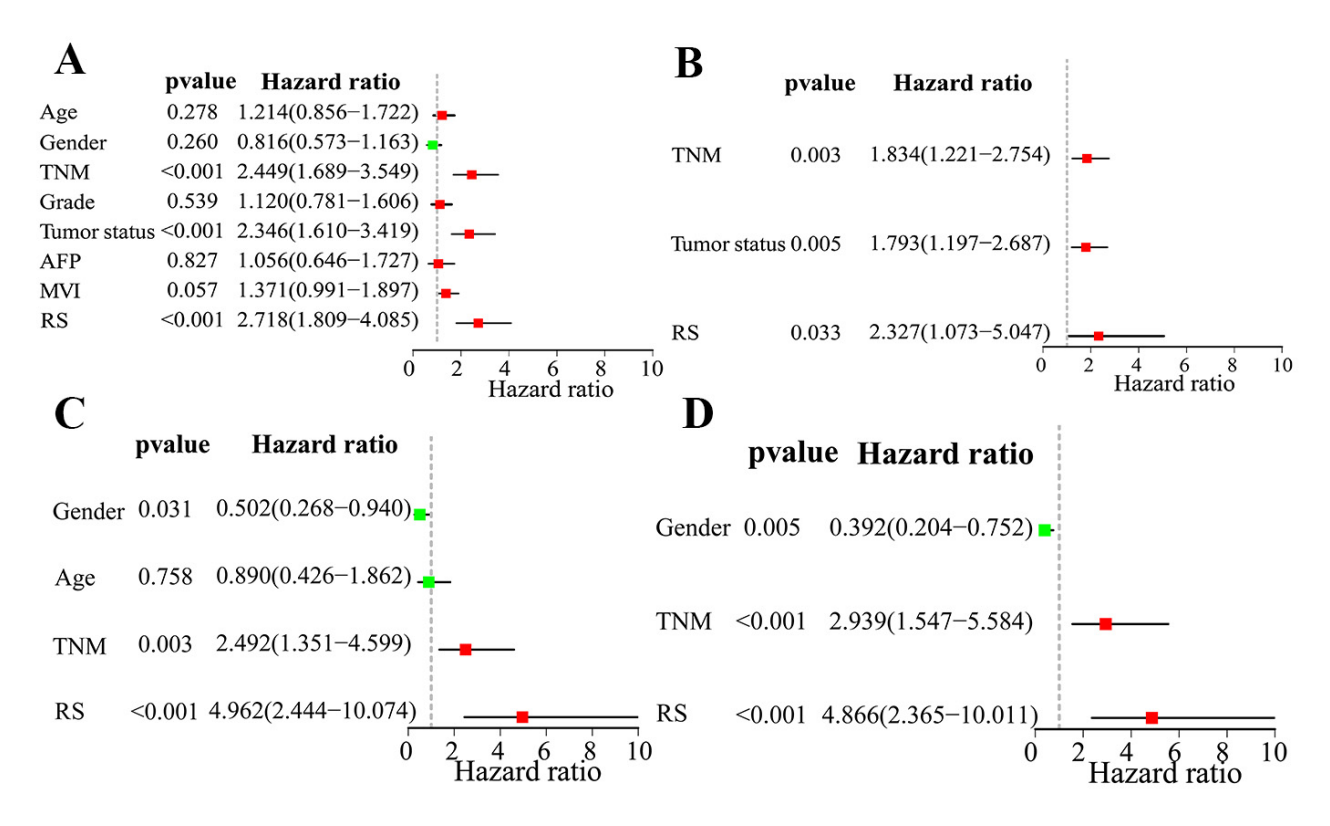


Fig. 5. Relation between the RS and clinical parameters (A–D). The TCGA and ICGC datasets both demonstrated that RS was a reliable prognostic biomarker.

cated that FBXOs may play a crucial role in the mitochondrial matrix and organic anion transmembrane transporter activity (**Supplementary Fig. 1C**). Through GSEA, we explored the differences in biological mechanisms and cancerrelated pathways between the subgroups. **Supplementary Fig. 1D** highlights the five pathways with the most noticeable inconsistencies. Notably, the cell cycle was significantly enriched in the high RS group.

3.7 RT-PCR Validation of Key Genes in HCC Tissues

To further evaluate the correlation between the key genes of the FBXO family and HCC, we collected 8 pairs of HCC and adjacent normal liver tissues, and their expression levels were detected by qRT-PCR. The results showed a significant increase in the expression of *CCNF*, *FBXO43*, and *FBXO45* in HCC compared to adjacent normal liver tissues (Fig. 8).

3.8 Knockdown of CCNF Suppresses the Proliferation of HCC

FBXO45 and FBXO43 can promote the malignant progression of HCC [18–21]. However, the biological function of CCNF in HCC remains unclear. We first detected the expression levels of CCNF in four HCC cell lines by qPCR. The results revealed the high expression of CCNF in Huh7 and HepG2 cells (Fig. 9A). To investigate the role of CCNF in HCC cell lines, we successfully transfected Huh7 and HepG2 with si-CCNF to knock down CCNF expres-

sion, confirmed by qPCR (Fig. 9B) and western blotting (Fig. 9C). Compared to the NC group, transfection of Huh7 and HepG2 cells with si-CCNF resulted in reduced proliferation (Fig. 9D–F) and colony-forming ability (Fig. 9G) (p < 0.05). These findings suggest that CCNF promotes the malignant development of HCC.

3.9 Genes Co-Expressed with CCNF in HCC and Functional Enrichment Analysis

In this study, we utilized cBioPortal and LinkedOmics online tools to screen the top 200 co-expressed genes with *CCNF*. As depicted in the Venn diagram in Fig. 10A, we obtained 166 overlapping genes. Subsequent GO enrichment analysis indicated that *CCNF* may play a specific role in processes such as nuclear division, DNA replication, spindle assembly, and DNA replication origin binding (Fig. 10B). Additionally, Kyoto Encyclopedia of Genes and Genomes (KEGG) analysis suggested the crucial involvement of *CCNF* in the cell cycle, DNA replication, and cellular senescence (Fig. 10C). These results indicate that *CCNF* may play a significant role in the development of HCC.

We employed a protein–protein interaction (PPI) network of 166 co-expressed genes with *CCNF* and identified key modules (**Supplementary Fig. 2**). Using cytoHubba in Cytoscape, we identified three hub genes closely associated with *CCNF*: cell division cycle protein 20 (CDC20), polo-like kinase 1 (PLK1), and cyclin-dependent kinase 1 (CDK1) (Fig. 10D). Further analysis using the GEPIA



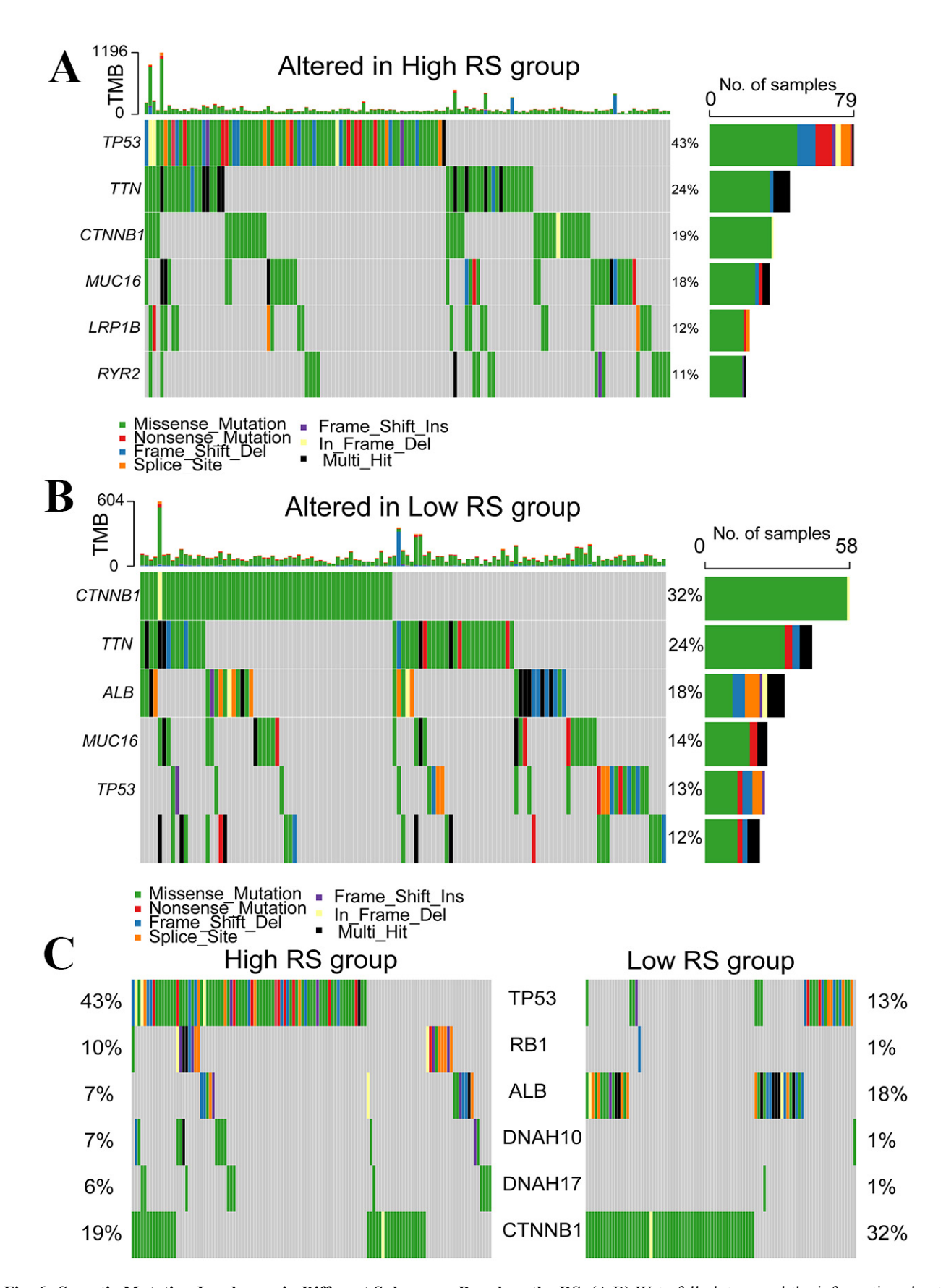


Fig. 6. Somatic Mutation Landscape in Different Subgroups Based on the RS. (A,B) Waterfall plots reveal the information about mutations in each HCC patient sample in the high and low RS groups. (C) Top 6 mutant genes displayed compared high or low RS group.

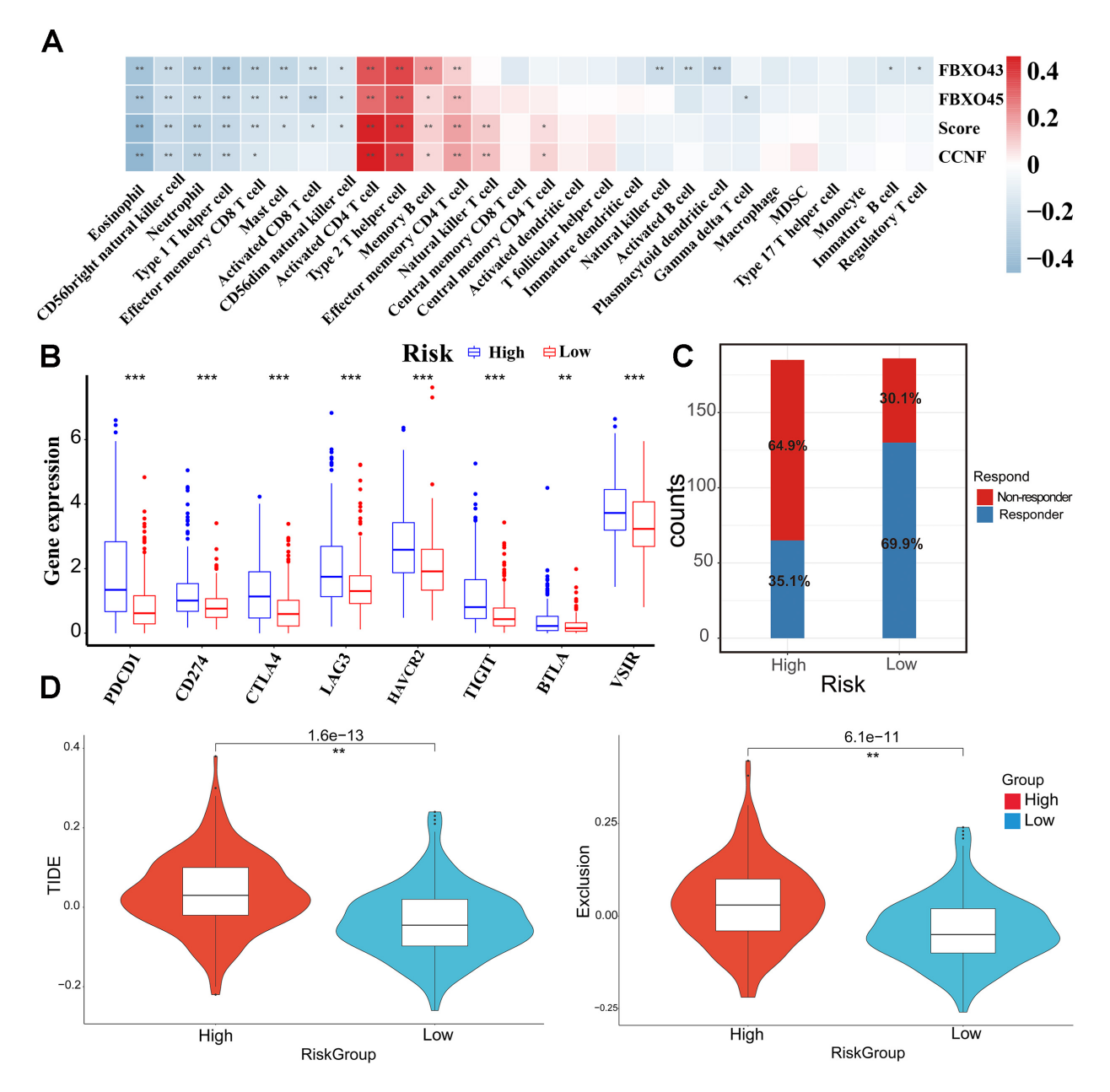


Fig. 7. The role of RS in immune responses in HCC. (A) Relationship between RS and 28 types of immune cells. (B) The relationships between the RS and various immune checkpoints. (C) TIDE analysis predicts the sensitivity of patients in high and low-RS groups to immunotherapy. (D) The difference in TIDE and Exclusion scores between high and low-RS groups. *p < 0.05, **p < 0.01, ***p < 0.001.

dataset (Fig. 10E) revealed a correlation between *CCNF* and these three central genes in HCC patients. Patients with higher levels of these hub genes had a poorer prognosis (Fig. 10F). These findings collectively suggest that *CCNF*, *CDC20*, *PLK1*, and *CDK1* may collaboratively contribute to the malignant progression of HCC.

4. Discussion

The advancement of bioinformatics tools allows researchers to identify reliable biological markers and build reliable cancer prognosis prediction signatures based on gene families. For instance, Fan *et al.* [22] developed a high-precision prognosis model based on the chemokine-and chemokine receptor gene family for predicting the clinical prognosis of lung adenocarcinoma patients. Yang *et al.* [23] incorporated lamin family genes into an HCC prognosis model. These signatures exhibit a favorable prognostic value for the OS of patients. TNM and Barcelona Clinic Liver Cancer stage are utilized to categorize HCC patients into different groups for corresponding treatments (e.g., surgery, radiation, immunotherapy). However, these methods are insufficient for providing individual prognostic predictions for patients [24,25]. Recent research indicates



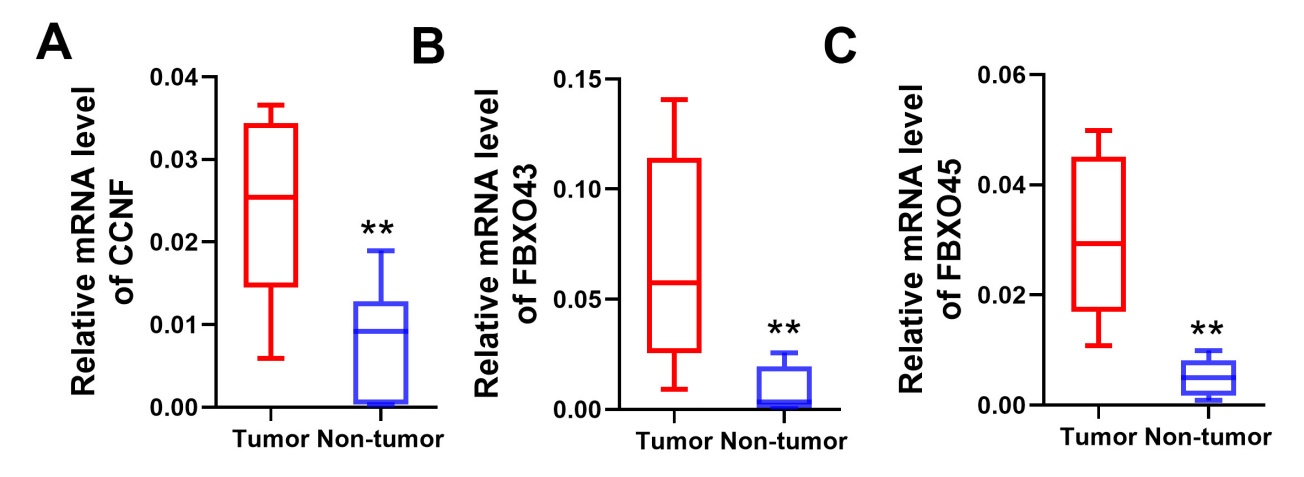


Fig. 8. Validation of CCNF, FBXO43, and FNXO45 expression levels in HCC tissues and normal liver tissues by qRT-PCR. (A–C) Box plots showing the expression levels of CCNF, FBXO43, and FBXO45 in HCC and normal liver tissues. Non-tumor: adjacent normal liver tissues (n = 8); tumor: HCC (n = 8). **p < 0.01. qRT-PCR, Quantitative Real-Time PCR.

that FBXO family members play a crucial role in tumor progression [18,26,27]. Nevertheless, the clinical value of FBXO family remains unclear. Therefore, we investigated the value of the FBXO family in predicting HCC prognosis and immune therapy responses.

We utilized bioinformatics tools to identify hub genes within the FBXO family and constructed a predictive model using hub genes (*CCNF*, *FBXO45*, and *FBXO43*). The model effectively identified high- and low-risk patients with differences in OS, clinicopathological characteristics, somatic mutations, and immune cell infiltration status. Finally, we investigated the biological function of *CCNF* in HCC cells, revealing *CCNF* as a potential therapeutic target for HCC.

Our study revealed that *CCNF*, *FBXO45*, and *FBXO43* are reliable biomarkers associated with adverse clinical outcomes in HCC. *CCNF* plays a key role in regulating various cellular processes, including maintaining genome stability, centrosome replication, DNA replication, and repair [10]. Studies suggest that the reduction of *CCNF* promotes cell senescence by CDK1 [28]. However, the biological functions of *CCNF* in HCC are still unclear. Our study found that *CCNF* is overexpressed in HCC, serving as an adverse prognostic factor for the disease. Targeting *CCNF* may be a promising approach for treating HCC. Additionally, we identified a gene cluster composed of *PLK1*, *CDK1*, and *CDC20*, which are significantly associated with *CCNF*. These genes may collaborate to promote the malignant progression of HCC.

FBXO43, a member of the F-box protein family [29], has been associated with a poor prognosis when overexpressed in HCC [30]. Studies suggest that FBXO43 deletion can suppress p53' proteasomal degradation and reduce ubiquitin-conjugating enzyme E2C expression, thereby preventing HCC cells from proliferating and invading surrounding tissues [19]. FBXO45, functioning as an E3 ligase substrate recognition subunit, has been implicated in vari-

ous human diseases including inflammation, malignancy, and nervous system disorders [27]. Abnormal expression of *FBXO45* has been associated with poor outcomes for patients [27]. A reduction of *FBXO45* consistently leads to the accumulation of p73 and eventually induces the death of affected cells [26]. However, other research suggests that *FBXO45* may block the epithelial–mesenchymal transition by targeting the transcription factors responsible for its initiation [31]. In summary, these findings indicate the potential of the FBXO family as a novel therapeutic target for HCC.

In our study, the analysis of somatic mutations in the high RS and low RS groups revealed that TP53 gene mutations were more common in the high RS group. TP53 is a crucial tumor suppressor gene, and mutations in the TP53 gene can reduce the anticancer capability of the p53 protein while conferring oncogenic properties [32]. TP53 mutations impact the anti-tumor immune response [33]. Therefore, for the high RS group, a more effective treatment strategy may involve directly targeting the mutated TP53 and restoring its wild-type function to inhibit the malignant progression of HCC [32].

The abundance of immune cell infiltration in HCC of the high-risk group was found to be lower compared to the low-risk group, indicating potential immunosuppression in these patients. Presently, immunotherapy has significantly improved the prognosis of liver cancer patients by enhancing the immune system. Clinically, immunotherapy drugs primarily target immune checkpoints for effective treatment, and routine assessment of immune checkpoints helps determine the suitability of patients for immunotherapy [34]. Additionally, the analysis revealed increased expression levels of immune checkpoint molecules, including CD274, HAVCR2, LAG3, VISIR, BTLA, and TIGIT, in high-risk liver cancer patients. These immune checkpoints are co-inhibitory receptors, and their high expression suggests T-cell dysfunction or exhaustion phenotypes and neg-



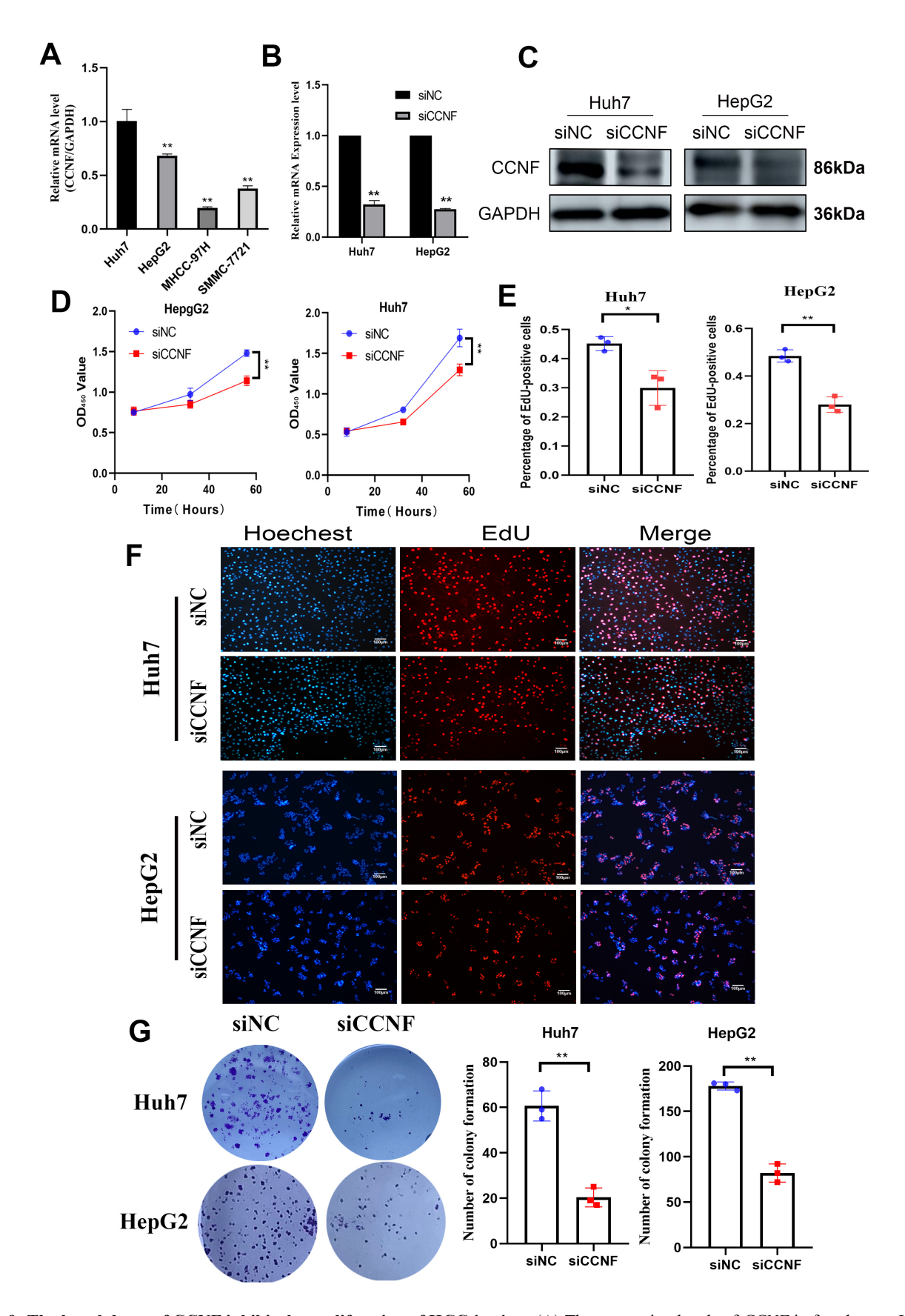


Fig. 9. The knockdown of CCNF inhibit the proliferation of HCC in vitro. (A) The expression levels of CCNF in four human HCC cell lines. (B,C) CCNF expression levels in control and siCCNF groups of HCC cell lines were detected using qRT-PCR (B) and Western blotting (C). (D–G) Knockdown of CCNF inhibit the proliferation of HCC cells in vitro, scale bars, $100 \, \mu m. *p < 0.05, **p < 0.01$.

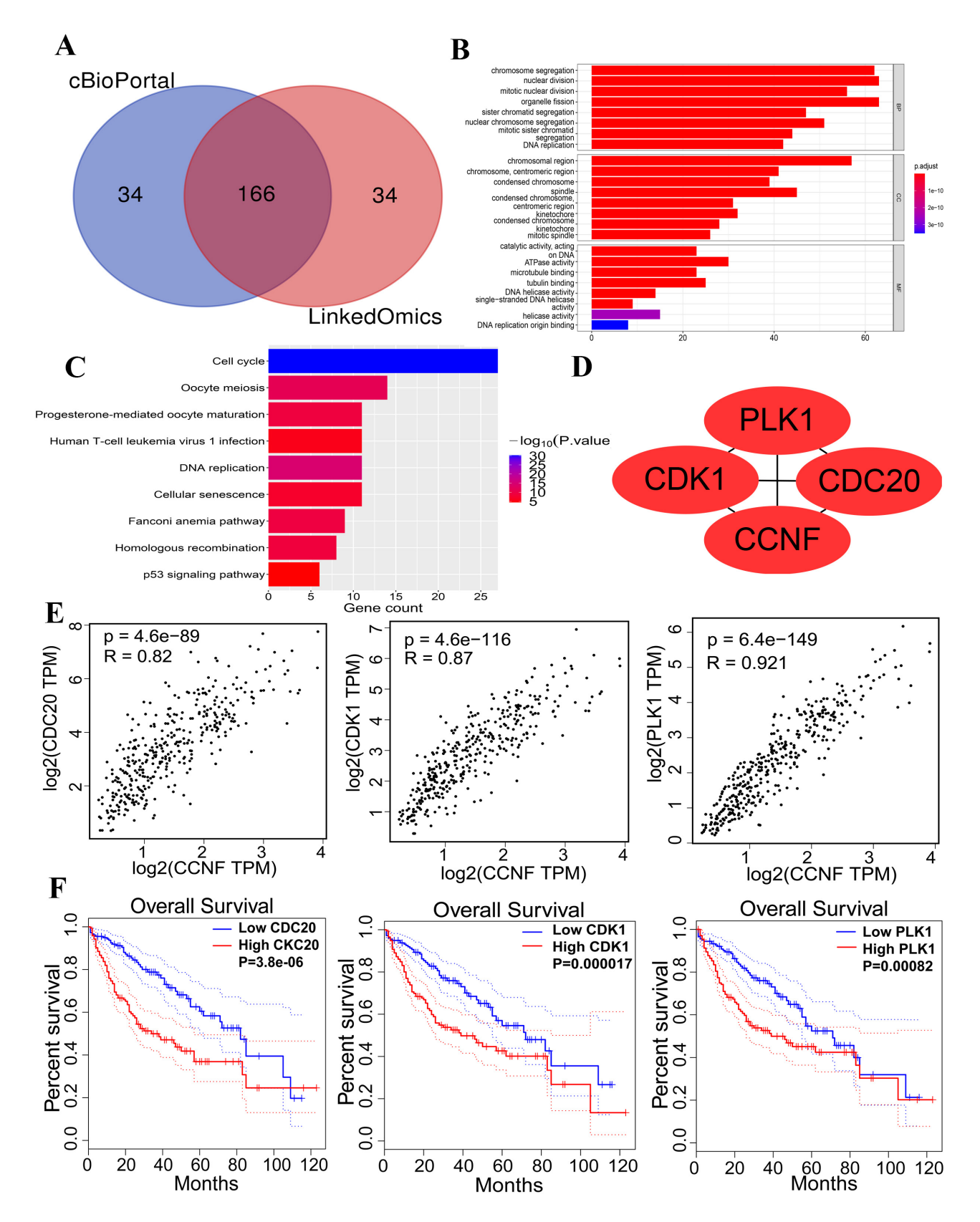


Fig. 10. PPI Network and bioinformatics Analysis of CCNF. (A) Intersection of genes that were got via the LinkedOmics and the cBioPortal database. (B,C) The GO and KEGG analysis were employed for predicted the functional of the *CCNF* and 166 co-expressed genes. (D) The hub-genes were distinguished via Cytoscape. (E) Correlation between 3 hub-genes and *CCNF* expression. (F) survival analyses of hub-genes in HCC.

ative regulation of anti-tumor responses [35]. Studies have shown significant therapeutic effects of these co-inhibitory receptors in the treatment of certain cancers [36]. Given the correlation between RS and these immune checkpoints, signature based on the FBXO family can be a promising tool to help identify liver cancer patients suitable for immunotherapy.

Presently, immunotherapy has significantly improved the prognosis of liver cancer patients by enhancing the immune system [23]. However, due to individual variations, the effectiveness of immunotherapy also varies among different populations. Therefore, it is crucial to determine which populations are more likely to benefit from immunotherapy. We evaluated the tumor immune microenvironment in TCGA cohort. The abundance of immune cell infiltration in HCC of the high-risk group was found to be lower compared to the low-risk group, indicating the potential immunosuppression in these patients. Clinically, immunotherapy drugs primarily target immune checkpoints for effective treatment, and routine assessment of immune checkpoints helps determine the suitability of patients for immunotherapy [34]. Through further TIDE analysis, we found that the TIDE and exclusion scores were significantly elevated in the high-risk group. The high-risk group exhibited a notably higher proportion of immunologically nonresponsive individuals, suggesting a greater propensity for immune escape and reduced responsiveness to immunotherapy. By contrast, the low-risk group appeared more suitable for immunotherapy [37]. Given the correlation between RS and the immunotherapy response, a signature based on the FBXO family could be a promising tool to help identify liver cancer patients suitable for immunotherapy.

This study had some limitations. First, external validation of the model through clinical trials is needed, and this study lacked a well-designed validation. Second, direct interactions between the FBXO family and immune cell infiltration need further clarification through more experiments. Third, further foundational experiments are needed to investigate the potential mechanisms by which *CCNF* promotes the progression of HCC.

5. Conclusions

The predictive model based on the FBXO family can effectively predict OS and the immune therapy response in HCC. Additionally, *CCNF* is a potential therapeutic target for HCC.

Abbreviations

TIDE, Tumor Immune Dysfunction and Exclusion; OS, Overall survival; WB, Western blotting; TNM, tumor-node-metastasis; DEGs, differentially expressed genes; CCNF, cyclin F; FBXO43, F-box protein 43; FBXO45, F-box protein 43.

Availability of Data and Materials

The study's original contributions presented in the study are included in the article or **Supplementary Material**. Any further questions could be directed to the corresponding author.

Author Contributions

XD and DG contributed to the study conception, design, and the whole process of article revision. DG, HG and SL performed the material preparation, data collection and analysis. DG, XL, and ZL performed the in vitro assays. LL and LB collect literature and draw charts. And all authors revised the manuscript and approved the final version. All authors have participated sufficiently in the work and agreed to be accountable for all aspects of the work.

Ethics Approval and Consent to Participate

The studies involving human participants were reviewed and approved by 2021-KY-1137-002, Ethics Committee of the First Affiliated Hospital of Zhengzhou University. The patients/participants provided their written informed consent to participate in this study.

Acknowledgment

We acknowledge assistance with the access of analytic instruments from the Department of Clinical Systems Biology Laboratories and Translational Medical Center at The First Affiliated Hospital of Zhengzhou University.

Funding

This work was supported by National Natural Science Foundation of China (82002560), Henan Provincial Science and Natural Science Foundation (232300420232) and Key Projects of Institutions of Higher Learning in Henan Province (21A320062).

Conflict of Interest

The authors declare no conflict of interest.

Supplementary Material

Supplementary material associated with this article can be found, in the online version, at https://doi.org/10.31083/j.fbl2905202.

References

- [1] Sung H, Ferlay J, Siegel RL, Laversanne M, Soerjomataram I, Jemal A, et al. Global Cancer Statistics 2020: GLOBOCAN Estimates of Incidence and Mortality Worldwide for 36 Cancers in 185 Countries. CA: A Cancer Journal for Clinicians. 2021; 71: 209–249.
- [2] Marasco G, Colecchia A, Colli A, Ravaioli F, Casazza G, Bacchi Reggiani ML, *et al.* Role of liver and spleen stiffness in predicting the recurrence of hepatocellular carcinoma after resection. Journal of Hepatology. 2019; 70: 440–448.



- [3] Kulik L, El-Serag HB. Epidemiology and Management of Hepatocellular Carcinoma. Gastroenterology. 2019; 156: 477– 491.e1.
- [4] Ren YD, Ye ZS, Yang LZ, Jin LX, Wei WJ, Deng YY, et al. Fecal microbiota transplantation induces hepatitis B virus e-antigen (HBeAg) clearance in patients with positive HBeAg after long-term antiviral therapy. Hepatology (Baltimore, Md.). 2017; 65: 1765–1768.
- [5] Huang YL, Ning G, Chen LB, Lian YF, Gu YR, Wang JL, et al. Promising diagnostic and prognostic value of E2Fs in human hepatocellular carcinoma. Cancer Management and Research. 2019; 11: 1725–1740.
- [6] Llovet JM, Castet F, Heikenwalder M, Maini MK, Mazzaferro V, Pinato DJ, et al. Immunotherapies for hepatocellular carcinoma. Nature Reviews. Clinical Oncology. 2022; 19: 151–172.
- [7] Ciechanover A. Intracellular protein degradation: From a vague idea thru the lysosome and the ubiquitin-proteasome system and onto human diseases and drug targeting. Best Practice & Research. Clinical Haematology. 2017; 30: 341–355.
- [8] Shapira M, Kakiashvili E, Rosenberg T, Hershko DD. The mTOR inhibitor rapamycin down-regulates the expression of the ubiquitin ligase subunit Skp2 in breast cancer cells. Breast Cancer Research: BCR. 2006; 8: R46.
- [9] Kuchay S, Giorgi C, Simoneschi D, Pagan J, Missiroli S, Saraf A, et al. PTEN counteracts FBXL2 to promote IP3R3- and Ca²⁺mediated apoptosis limiting tumour growth. Nature. 2017; 546: 554-558
- [10] D'Angiolella V, Donato V, Forrester FM, Jeong YT, Pellacani C, Kudo Y, et al. Cyclin F-mediated degradation of ribonucleotide reductase M2 controls genome integrity and DNA repair. Cell. 2012; 149: 1023–1034.
- [11] Hsu JY, Reimann JDR, Sørensen CS, Lukas J, Jackson PK. E2F-dependent accumulation of hEmi1 regulates S phase entry by inhibiting APC(Cdh1). Nature Cell Biology. 2002; 4: 358–366.
- [12] Yang H, Xu Z, Xu X, Rahman MM, Li X, Leng X. Transcriptomic and biochemical analyses revealed the improved growth, lipid metabolism, and flesh quality of grass carp (Ctenopharyngodon idellus) by dietary Eucommia ulmoides bark and leaf supplementation. Journal of Animal Science. 2022; 100: skac250.
- [13] Tang Z, Li C, Kang B, Gao G, Li C, Zhang Z. GEPIA: a web server for cancer and normal gene expression profiling and interactive analyses. Nucleic Acids Research. 2017; 45: W98–W102.
- [14] Zhao F, Su L, Wang X, Luan J, Zhang X, Li Y, *et al.* Molecular map of disulfidptosis-related genes in lung adenocarcinoma: the perspective toward immune microenvironment and prognosis. Clinical Epigenetics. 2024; 16: 26.
- [15] Dang XW, Pan Q, Lin ZH, Wang HH, Li LH, Li L, et al. Overexpressed DEPDC1B contributes to the progression of hepatocellular carcinoma by CDK1. Aging. 2021; 13: 20094–20115.
- [16] Li L, Li S, Wang H, Li L, Wang P, Shen D, et al. GSG2 promotes tumor growth through regulating cell proliferation in hepatocellular carcinoma. Biochemical and Biophysical Research Communications. 2022; 625: 109–115.
- [17] Cheu JWS, Wong CCL. Mechanistic Rationales Guiding Combination Hepatocellular Carcinoma Therapies Involving Immune Checkpoint Inhibitors. Hepatology (Baltimore, Md.). 2021; 74: 2264–2276.
- [18] Li CM, Zhang J, Wu W, Zhu Z, Li F, Wu D, et al. FBXO43 increases CCND1 stability to promote hepatocellular carcinoma cell proliferation and migration. Frontiers in Oncology. 2023; 13: 1138348
- [19] Zhou H, Zeng C, Liu J, Luo H, Huang W. F-Box Protein 43, Stabilized by N6-Methyladenosine Methylation, Enhances Hepatocellular Carcinoma Cell Growth and Invasion via Promoting p53 Degradation in a Ubiquitin Conjugating Enzyme E2 C-Dependent Manner. Cancers. 2023; 15: 957.
- [20] Lin XT, Yu HQ, Fang L, Tan Y, Liu ZY, Wu D, et al. Ele-

- vated FBXO45 promotes liver tumorigenesis through enhancing IGF2BP1 ubiquitination and subsequent PLK1 upregulation. eLife. 2021; 10: e70715.
- [21] Zhang Y, Wang JW, Su X, Li JE, Wei XF, Yang JR, et al. F-box protein 43 promoter methylation as a novel biomarker for hepatitis B virus-associated hepatocellular carcinoma. Frontiers in Microbiology. 2023; 14: 1267844.
- [22] Fan T, Liu Y, Liu H, Wang L, Tian H, Zheng Y, et al. Comprehensive analysis of a chemokine- and chemokine receptor family-based signature for patients with lung adenocarcinoma. Cancer Immunology, Immunotherapy: CII. 2021; 70: 3651–3667.
- [23] Yang Y, Xiao W, Liu R, Gao L, Chen J, Kan H. A Lamin Family-Based Signature Predicts Prognosis and Immunotherapy Response in Hepatocellular Carcinoma. Journal of Immunology Research. 2022; 2022: 4983532.
- [24] Duseja A. Staging of hepatocellular carcinoma. Journal of Clinical and Experimental Hepatology. 2014; 4: S74–9.
- [25] Liu H, Yan Y, Chen R, Zhu M, Lin J, He C, et al. Integrated nomogram based on five stage-related genes and TNM stage to predict 1-year recurrence in hepatocellular carcinoma. Cancer Cell International. 2020; 20: 140.
- [26] Peschiaroli A, Scialpi F, Bernassola F, Pagano M, Melino G. The F-box protein FBXO45 promotes the proteasome-dependent degradation of p73. Oncogene. 2009; 28: 3157–3166.
- [27] Lin M, Wang ZW, Zhu X. FBXO45 is a potential therapeutic target for cancer therapy. Cell Death Discovery. 2020; 6: 55.
- [28] Li X, Li YJ, Wang MJ, Ou KP, Chen YQ. Inhibition of Cyclin F Promotes Cellular Senescence through Cyclin-dependent Kinase 1-mediated Cell Cycle Regulation. Current Medical Science. 2023; 43: 246–254.
- [29] Tung JJ, Hansen DV, Ban KH, Loktev AV, Summers MK, Adler JR, 3rd, et al. A role for the anaphase-promoting complex inhibitor Emi2/XErp1, a homolog of early mitotic inhibitor 1, in cytostatic factor arrest of Xenopus eggs. Proceedings of the National Academy of Sciences of the United States of America. 2005; 102: 4318–4323.
- [30] Wu S, Qin L, Yang J, Wang J, Shen Y. Association between F-box-only protein 43 overexpression and hepatocellular carcinoma pathogenesis and prognosis. Cancer Medicine. 2023; 12: 10062–10076.
- [31] Xu M, Zhu C, Zhao X, Chen C, Zhang H, Yuan H, *et al.* Atypical ubiquitin E3 ligase complex Skp1-Pam-Fbxo45 controls the core epithelial-to-mesenchymal transition-inducing transcription factors. Oncotarget. 2015; 6: 979–994.
- [32] Hu J, Cao J, Topatana W, Juengpanich S, Li S, Zhang B, *et al.* Targeting mutant p53 for cancer therapy: direct and indirect strategies. Journal of Hematology & Oncology. 2021; 14: 157.
- [33] Li L, Li M, Wang X. Cancer type-dependent correlations between TP53 mutations and antitumor immunity. DNA Repair. 2020; 88: 102785.
- [34] Gibney GT, Weiner LM, Atkins MB. Predictive biomarkers for checkpoint inhibitor-based immunotherapy. The Lancet. Oncology. 2016; 17: e542–e551.
- [35] Anderson AC, Joller N, Kuchroo VK. Lag-3, Tim-3, and TIGIT: Co-inhibitory Receptors with Specialized Functions in Immune Regulation. Immunity. 2016; 44: 989–1004.
- [36] Shi X, Li CW, Tan LC, Wen SS, Liao T, Zhang Y, et al. Immune Co-inhibitory Receptors PD-1, CTLA-4, TIM-3, LAG-3, and TIGIT in Medullary Thyroid Cancers: A Large Cohort Study. The Journal of Clinical Endocrinology and Metabolism. 2021; 106: 120–132.
- [37] Taki M, Abiko K, Ukita M, Murakami R, Yamanoi K, Yamaguchi K, et al. Tumor Immune Microenvironment during Epithelial-Mesenchymal Transition. Clinical Cancer Research: an Official Journal of the American Association for Cancer Research. 2021; 27: 4669–4679.

